The Structure of an East Australian Current Anticyclonic Eddy

JOHN C. ANDREWS

Australian Defence Scientific Service, Department of Defence, Weapons Research Establishment, Salisbury, South Australia

PAUL SCULLY-POWER

Royal Australian Navy Research Laboratory, Garden Island, New South Wales, Australia

(Manuscript received 22 July 1975, in revised form 25 February 1976)

ABSTRACT

An intense, anticyclonic, warm core winter eddy off the east coast of Australia was surveyed with an airborne radiation thermometer, expendable bathythermographs and a continuously recording surface thermosalinograph in September 1974. The eddy had a diameter of 250 km, a dynamic relief of 0.7 dyn-m and a mixed layer depth extending to over 300 m in the core. A strong current ring was present halfway from the center to the edge of the eddy with surface speeds ranging from 0.6 to 1.78 m s^{-1}. The dynamics of the eddy are related to previous knowledge of mesoscales in the East Australian Current region. The simplicity of the eddy structure defines a dominant and lone horizontal wavenumber whose inverse is the Rossby radius of deformation predicted by complex baroclinic instability theory. This simplicity allows a very simple eddy model to be proposed with first vertical baroclinic mode structure with a vertical depth scale of 430 m. The interior deep mixed layer was completely enclosed by a shell of isothermal water; this double layering indicates that large-scale entrainment of surface water may be an important feature of eddy generation off East Australia.

1. Introduction

Warm core eddies off East Australia have been observed from time to time but on no occasion has the station coverage been adequate to resolve the structure of an eddy. Hamon (1961) reported the southerly current observed within 60 mi of the continental shelf coexists with a northeasterly "countercurrent" further offshore, suggesting that anticyclonic eddies may be a feature of the general circulation. Wyrtki (1962) produced dynamic topographies of the southwest Pacific which suggested that these eddies are separated from the main current and probably drift south down the coast. In 16 maps of dynamic topography covering various portions of the area from 20° to 40°S, Hamon (1965) and Boland and Hamon (1970) showed mainly south-directed baroclinic waves north of about 30°–33°S and some closed circular eddies south of about 34°S. Eddy diameters ranged from about 200–250 km while drift rates were estimated to lie within about 5–8 km day^{-1}. Hynd (1969) tracked a "pool of warm water" with an airborne radiation thermometer (ART) for a month in midsummer, finding a drift rate of 5.5 km day^{-1}. The pool was about 50–70 km in diameter and was surrounded by marked temperature fronts. Boland (1973) presented the results of two years of west-east expendable bathythermograph (XBT) sections across the Tasman Sea at 33.5°S. He found that the average time between the appearance of successive eddy structure on the section was about 73 days and that strong currents appear and disappear within 40-day intervals. If the south-directed baroclinic waves mature into more circular eddies around latitude 34°S, then their formation time from the appearance of the East Australian Current on Boland's section to the disappearance from the section of the two arms of the current ring is equated to the 40 days. Hamon and Cresswell (1972) deduced a dominant length scale (distance between like eddies) of 500 km from structure function analysis; combined with a time scale of 73 days, this yields a southward drift of about 7 km day^{-1}. Hamon (1962, 1968a) found an anomalous peak in the mean sea level spectra at Sydney, Coff's Harbour and Lord Howe Island in the frequency range corresponding to periods from 20 to 50 days which may be associated with the moving circulation patterns; the drift rates for eddies of diameters 200–250 km would be 5–10 km day^{-1}.

The general picture obtained from the literature on the East Australian Current is that circular anticyclonic eddies are formed between about 30°–35°S from baroclinic perturbations with anticyclonic vorticity which migrate down the coast from about 20°S in the southern Coral Sea (Scully-Power, 1973). The diameters are about 200–250 km and the drift rates are about 5–10 km day^{-1}.

2. The nature of the experiment

In order to examine this system further an attempt was made to locate and to delineate an anticyclonic

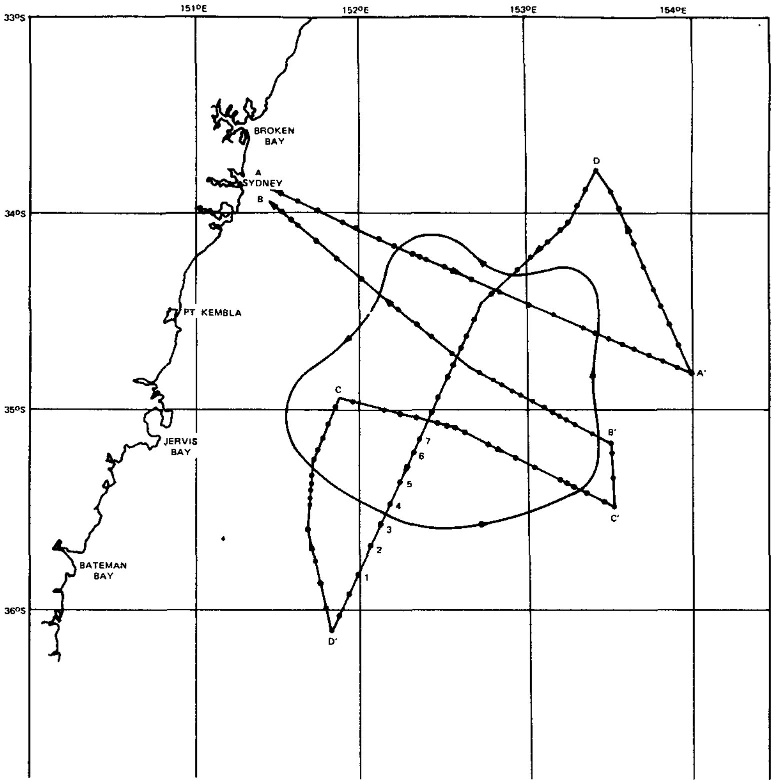

FIG. 1. Cruise track showing XBT stations and the core of the eddy current (10–13 September 1974).

eddy off the east coast of Australia in September 1974. Three ART surveys at 14-day intervals immediately prior to the cruise indicated that an anticyclone was bounded by 34° and 36°S and by 154°E and the coast. The dots on the cruise track (HMAS *Kimbla*, 9–13 September 1974, Fig. 1) show positions where XBT traces were taken to 450 m. Surface water temperature and salinity (±0.1°C, ±0.03‰) were monitored continuously around the track. Fig. 1 also shows the core of the eddy current[1] and reflects the strategy adopted in continually varying the cruise track in order fully to delineate the eddy in the shortest possible time. No other data were contemplated since temperature is the main factor governing density off East Australia (Hamon, 1968b).

3. Surface temperature

The main features of surface temperature in relation to the eddy are shown in Fig. 2. Surface thermal fronts from four ART surveys and from the shipborne thermosalinograph have been inserted and the dotted line shows the core of the eddy current. Thus considerable frontal structure surrounds the quiescent core of the eddy which has an anomalously high temperature of 2–3°C relative to the water beyond the core of the current. The solid line shows the center of a tongue of warm (19–21°C) northern water advected around the western edge of the eddy. The boundary between the anomalously warm core and tongue and the cooler surrounding water (15–18°C) is approximately the 18°C isotherm of the ART survey of 3–5 September 1974. This is shown as the dashed line in Fig. 2.

4. Temperature at depths of 240 and 400 m

Hamon (1968b) showed that a strong correlation existed between the temperature at 240 m ($T240$) and the dynamic height of the sea surface relative to the 1300 db level [$\eta(0/1300)$]. His regression relation for winter is

$$\eta = 0.089\, T240 + 0.441 \quad [\text{dyn-m, °C}]. \qquad (1)$$

Fig. 3 shows isotherms at 240 m and in the light of (1), it is essentially a map of the dynamic height of the sea surface. A well-defined anticyclonic eddy is shown with peripheral structure of length scale about 30 km; this smaller scale structure was noted by Hamon (1970). The largely isothermal core at about 18°C is the result

[1] The eddy core is the relatively quiescent body of water enclosed by the zone of fastest flowing surface water. The isopleth of highest surface speed is termed the core of the eddy current. The azimuthal velocity increases radially from zero in the center of the eddy to a maximum in the core of the eddy current. Beyond the core of the eddy current the azimuthal velocity decreases again to zero.

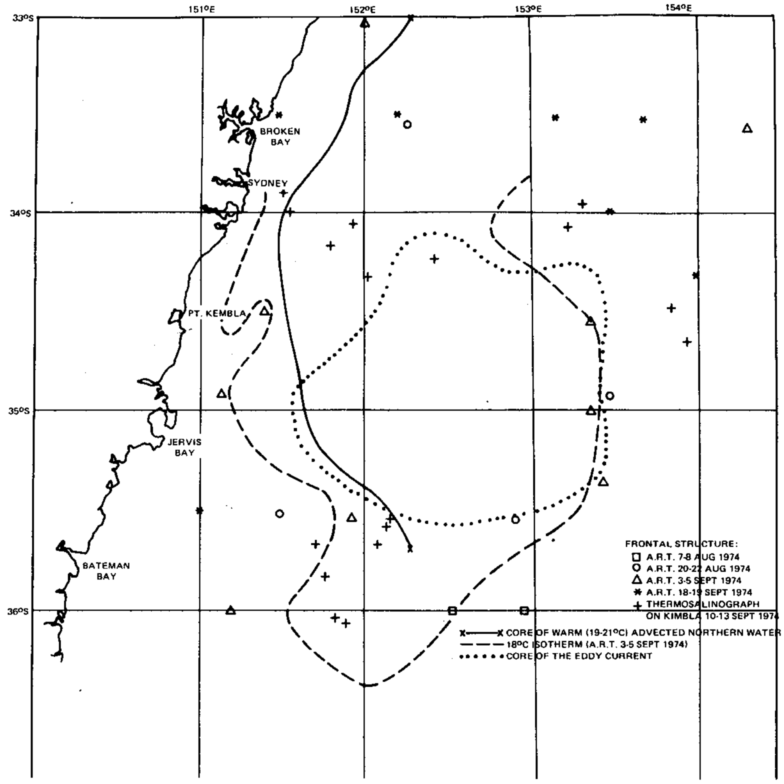

FIG. 2. Highlights of remote (ART) sensing of the sea surface temperature.

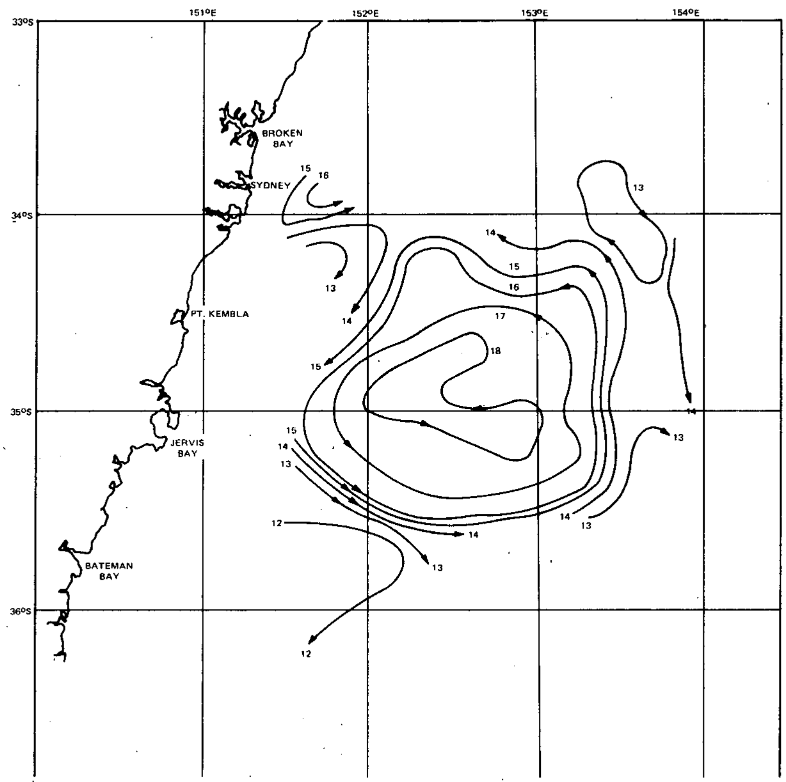

FIG. 3. Isotherms (°C) at 240 m depth.

of the penetration of surface isothermal water beyond 240 m depth. The East Australian Current is seen by the crowding of the isotherms about 90 km from the coast while the "countercurrent" flows due north at about 153.4°E.

The isotherms at 400 m depth (not shown here) mirror Fig. 3 to a remarkable degree; the thermal range in *T*400 (6–8°C) is greater than in *T*240 (5–6°C) in crossing the eddy and the small-scale peripheral structure at 400 m also shows greater relief than at 240 m. Since the vertical gradient of temperature is greater at 240 m than at 400 m and the horizontal gradient of temperature is less at 240 m than at 400 m, we may conclude that the downward displacement of isotherms increases with depth, at least in the top 400 m. Bye (1972) noted a maximum oscillation at 900 m depth in the Rossby wave system to the south of Australia. Finally, the diameter of the current ring is the same at 240 m as at 400 m.

5. Surface and subsurface mixed layers

Contours of mixed layer depth are shown in Fig. 4 and it is immediately evident on comparing Figs. 3 and 4 that the most striking feature of our eddy is the very deep core of surface mixed water. Since the small-scale peripheral structure is present in Fig. 4 and in the fields of *T*240 and *T*400, it may be an integral part of the total eddy structure; it has a wavelike nature which is consistent with an eddy model presented in Section 8.

A second mixed layer was found beneath the 18°C (approximately) isothermal surface layer on all but 4 of the 115 XBT traces and has a temperature of 16.75°C. Fig. 5 shows the temperature section along the diameter DD′ of Fig. 1 and the 16.75°C layer is evidenced by the wide spacing between the 16°C and 17°C isotherms. The surface layer is evidently completely encapsulated by the 16.75°C layer; the thickness of the latter layer varies in a regular manner from 70 m at the centre of the eddy to 10 m at the core of the eddy current. Beyond the core of the eddy current the thickness increases to the point where the 16.75°C layer actually becomes the surface layer at distances of about 25 and 250 km from D. Other sections (AA′, BB′, CC′ on Fig. 1) show the same type of behavior.

This suggests a large-scale entrainment of warm northern water as the eddy is formed. Godfrey (1973b) has shown that Coral Sea surface water is uplifted over cooler southern surface water and carried south with the near-coastal East Australian Current. Fig. 2 shows just such a warm tongue advected around the eddy. It is likely that this warmer northern water is entrained into the void left by the downwelling vortex tube over the original 16.75°C mixed layer. In some respects this is similar to the cold-core current rings formed from meanders of the Gulf Stream, where a ring of Gulf

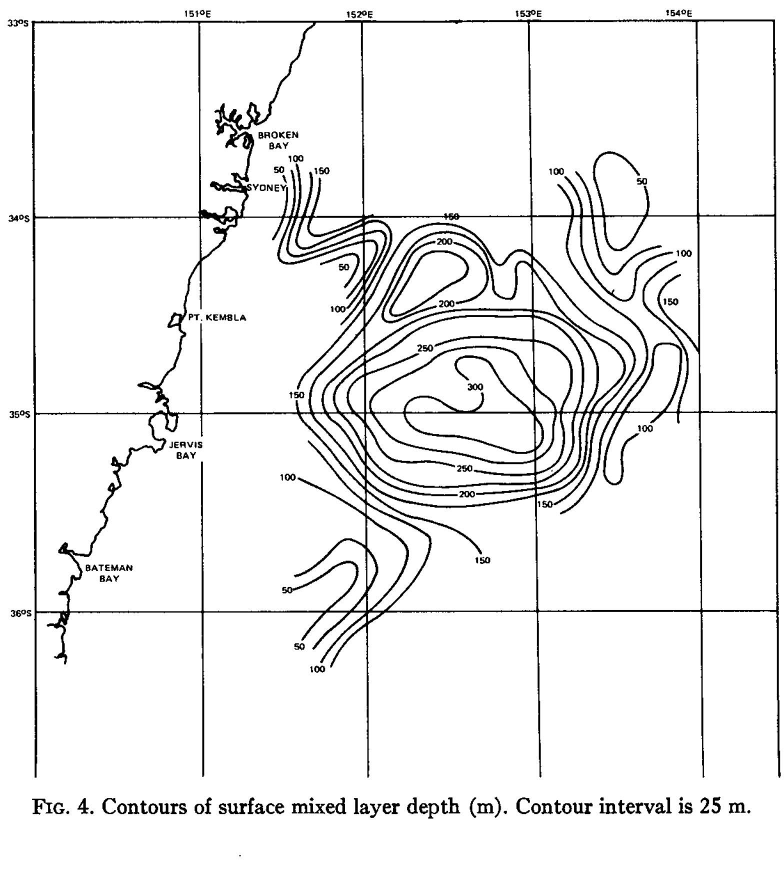

FIG. 4. Contours of surface mixed layer depth (m). Contour interval is 25 m.

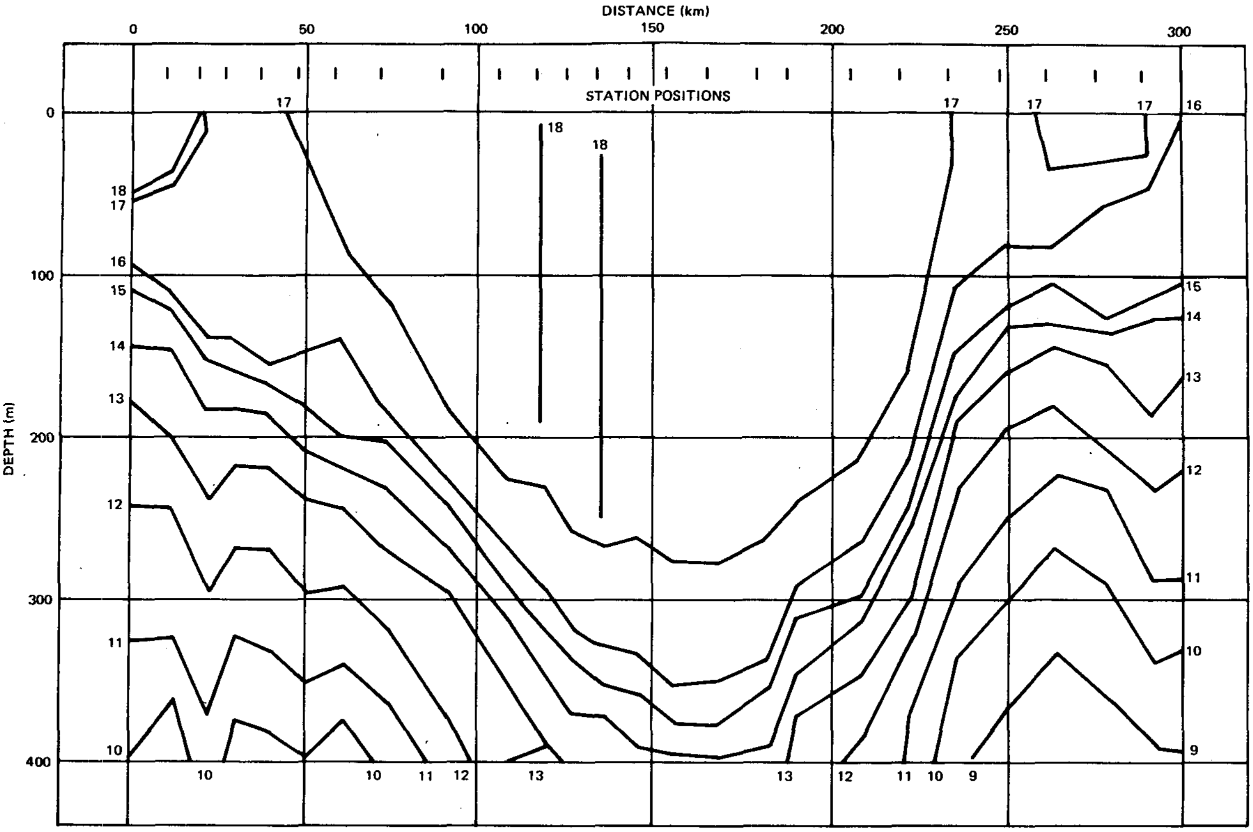

FIG. 5. Temperature section along DD′ (Fig. 1).

Stream water is detached from the main stream after enclosing a segment of colder slope water and forms a current ring embedded in Sargasso Sea water (e.g., Fugilister, 1972). We emphasize that the two processes are quite different and that it is probably dangerous at this stage to try to compare East Australian Current anticyclonic rings with Gulf Stream cyclonic rings. Kuroshio anticyclonic eddies (e.g., Kitano, 1974) do exhibit downwelling in their centers but this downwelling decreases rapidly toward the surface so that the surface layer structure is quite unlike that reported here.[2]

6. Frontal structure and eddy length scales

The crowding of the isopleths at an intermediate distance from the eddy center (Figs. 3 and 4) indicates the frontal nature of the eddy structure as well as its axial symmetry. Fig. 6 shows *T*240, *T*400 and mixed layer depth along the diameter DD′ of Fig. 1 and the frontal structure emerges as the strong horizontal gradients of these parameters centered at about 90 and 220 km from D. These are also the positions of maximum gradient on Fig. 5, so the diameter of the current ring on the section parallel to the coast is 130 km; on the sections perpendicular to the coast (BB′ and CC′ of Fig. 1, not shown here) the same figure of 130 km is found for the ring diameter.

We now consider the eddy diameter which is quite different from the diameter of the current ring. The center of the disturbance is located on Figs. 5 and 6 at a distance of 160 km from D while the eddy radii (zero horizontal gradient) lie at about 30 and 260 km from D. Thus the diameter of the eddy on the section DD′ is 230 km, the same as the diameter deduced from sections BB′ and CC′ (not shown) perpendicular to the coast. The diameter of the axially symmetric eddy is approximately twice the diameter of the current ring formed by the core of the eddy current.

The change in the thermal profiles in crossing the front on the southern half of section DD′ is shown in Fig. 7; profiles 1–3 are outside the core of the eddy current while profiles 4–7 are inside the quiescent core of the eddy. The current ring itself is largely the result of the difference in density between, say, profiles 3 and 4. Profiles 1–7 indicate horizontal temperature gradients across the front which increase with depth, at least to

[2] *Note added in proof:* We have recently discovered a flat spot near 16.7°C on the precision potentiometer of the XBT recorder used in this paper and thus we can only say definitively that the thickness of this sublayer is a good indicator of the local temperature gradient at that point, with thicker regions indicating lower gradients. (We are indebted to Dr. C. S. Nilsson for his assistance on the determination of this effect.)

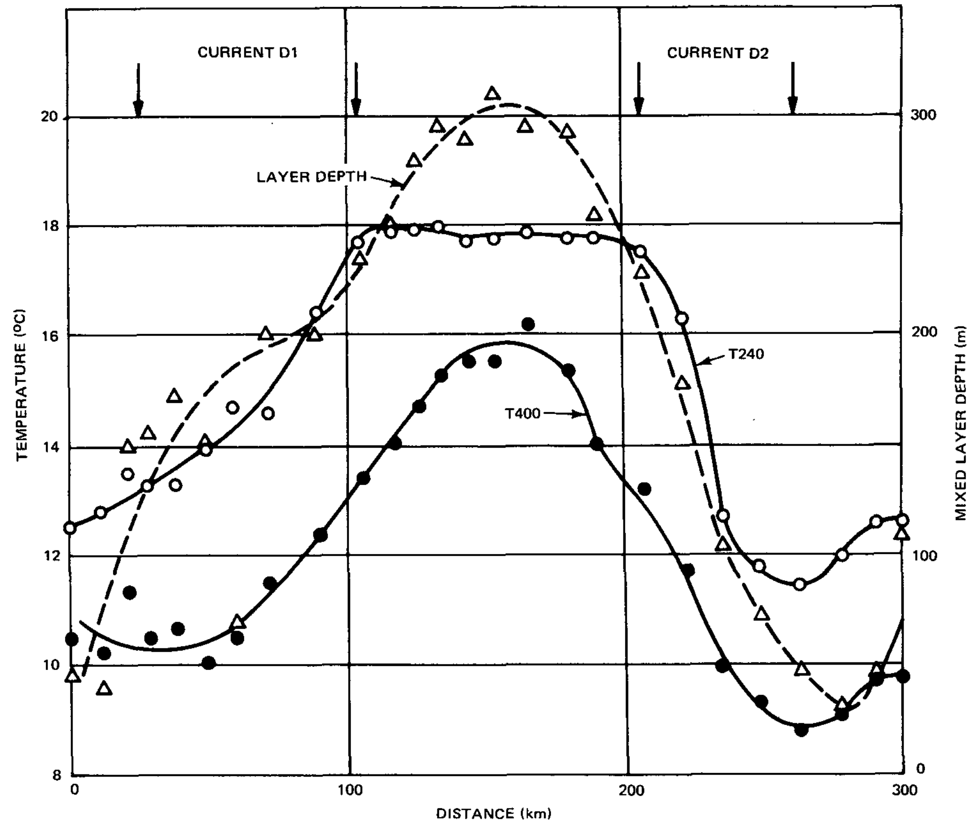

FIG. 6. Eddy structure along section DD′ (Fig. 1).

400 m, to such an extent that the horizontal change in temperature at 400 m is 30% of the total vertical change in temperature from the ocean surface to the ocean floor. Even so the thermal gradient across the fronts in our eddy is gentler than in Kuroshio anticyclonic eddies (Kitano, 1974) and in Gulf Stream cyclonic rings (Fugilister, 1972). In addition, the frontal structure to the north in Fig. 5 is even weaker than that to the south.

7. Eddy currents

The core of the eddy current has been defined as the region of fastest flowing surface current. Boland (1973) defines the core of the East Australian Current in terms of the 15°C isotherm at 240 m depth and it is this isotherm which has been inserted on Figs. 1 and 2 to represent the current core. It is obvious from the gradients on Figs. 3, 5, 6 and 7 that Boland's definition applies to our eddy as well.

The current structure can be estimated from the gradients of $T240$ across the eddy sections; for example, in Fig. 6 there are two well-defined currents designated D1 and D2 in the top of the figure with widths delineated by the arrows. The current speeds can be estimated from (1) and the geostrophic relation to give currents components at right angles to the cruise track. The actual bearings of the currents can be estimated from the streamlines of the 14°C, 15°C and 16°C isotherms in Fig. 3, so true currents and widths can be adjusted trigonometrically. This was done for the

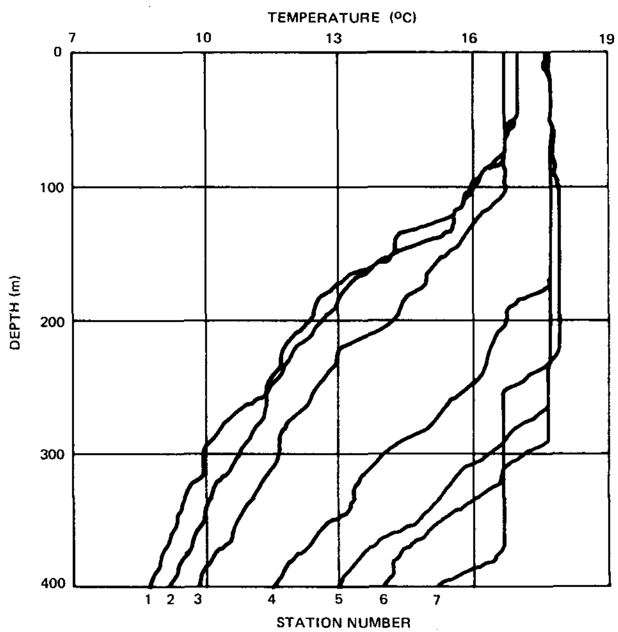

FIG. 7. Temperature profiles across the core of the eddy current at stations 1–7 on section DD′ (Fig. 1).

various sections on Fig. 1 and the greatest adjustment was 13%. The results are presented in Fig. 8 with the current widths superimposed across the core of the eddy current and joined by the dotted lines to show the probable bounds of the current. The speeds vary from 0.6 to 1.8 m s^{-1} and the current is about 40–80 km wide, being narrowest and fastest in the southeast sector. The East Australian Current and the Countercurrent in this instance are simply the western and eastern expression of a current ring.

8. A rudimentary model for East Australian eddies

Figs. 3–6 show an axially symmetric structure which is quite uncomplicated and appears to have only one horizontal wavenumber. It is possible that it may be described by a simple "bell-shaped" topography such as the Gaussian function Patzert (1969) used for Hawaiian eddies. Regardless of the horizontal function, a vertical baroclinic mode will be associated with it and it will have a vertical wavenumber D^{-1} related to the horizontal wavenumber k through the density stratification. Lighthill (1969) suggested that the group velocity of large wavelength baroclinic Rossby waves falls off so rapidly for high order modes in western boundary currents that the velocity structure should be predominantly of the first internal baroclinic mode. A differential equation for the velocity profile involving the density gradient and a scale depth H_n to be determined as an eigenvalue was proposed. Godfrey (private communication) found a good analytic approximation to the density structure near Sydney and was able to solve Lighthill's equation analytically. Thus he obtained the Rossby radii of deformation for all modes solely from the density structure; for the first mode he found the radius of deformation to be $\mu = 39.6$ km. He only presented the velocity profile for the first mode in his paper on East Australian eddies and found good agreement with measured geostrophic profiles [Figs. 3 and 4 of Godfrey (1973b)]. More importantly, he found that the group velocities of higher order modes (private communication) fell off rapidly; for $n = 1, 2, 3, 4, \ldots$ he found $V_g = 2.7, 0.74, 0.33, 0.19$ cm s^{-1} .... Thus Godfrey has offered the reason why our eddy apparently has only one horizontal wavenumber.

We have been able to derive Lighthill's equation for the velocity profile on a constant f plane from a simple vorticity argument and have arrived at an explicit formula for H_1 (higher modes are not possible on a constant f plane) in terms of k and f by extending Rhines' (1970) theory of inertio-gravity waves.

Consider an infinitesimally thin layer of initially horizontal fluid of thickness ΔZ_0 in an unperturbed, continuously stratified ocean with zero baroclinic velocity. Now an axially symmetric perturbation causes the isopycnals to rise a height ϵ above their equilibrium height. As vortex stretching takes place an azimuthal

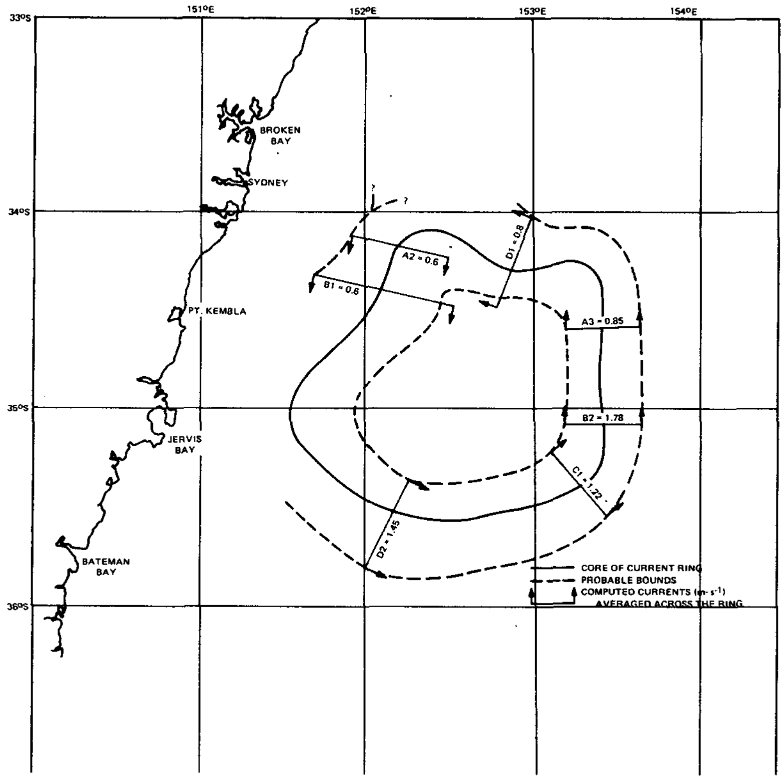

FIG. 8. Surface current distribution.

mesoscale current develops and the vorticity conservation equation is

$$\left(\frac{1}{r}\frac{\partial}{\partial r}rv+f\right)\Big/(\Delta Z_0+\Delta\epsilon)=f/\Delta Z_0, \quad (2)$$

where $\Delta\epsilon$ is the difference in ϵ at the top and bottom of the thin layer. Since $\Delta\epsilon\approx(\partial\epsilon/\partial z)\Delta Z_0$, Eq. (2) becomes

$$\frac{1}{r}\frac{\partial}{\partial r}rv=f\frac{\partial\epsilon}{\partial z}. \quad (3)$$

By definition the density change following an isopycnal is zero. If density is divided into the undisturbed part $\bar{\rho}$ and the perturbation due to vertical advection ρ', it is possible to show, after noting that initially $\rho'=0$ and that $\bar{\rho}\gg\rho'$ always, that

$$\rho'\approx-\epsilon\frac{\partial\bar{\rho}}{\partial z}, \quad (4)$$

where z is measured upward from the free sea surface. The perturbation pressure p' is the vertical integral of $\rho' g$ with respect to z and for a baroclinic disturbance, where $v(z)\rightarrow 0$ as $z\rightarrow-\infty$, the perturbation pressure becomes

$$p'=-\rho\int_{-\infty}^{z}\epsilon N^2 dz, \quad (5)$$

where N is the Brunt-Väisälä frequency. Using the geostrophic approximation to derive v from p' and inserting the result in (3) gives the eigenequation for ϵ. Differentiating this result with respect to z gives the convenient form

$$\frac{1}{r}\frac{\partial}{\partial r}r\frac{\partial\epsilon}{\partial r}=(f/N)^2\frac{\partial^2\epsilon}{\partial z^2}. \quad (6)$$

Seek separable solutions for $\epsilon(r,z)$ of form $\epsilon=G(z/D)J(kr)$, where k is the horizontal wavenumber and D^{-1} the vertical wavenumber. The result is

$$J=J_0(kr),\quad \frac{\partial^2 G}{\partial(z/D)^2}=(DkN/f)^2 G. \quad (7a,b)$$

Here $J_0(kr)$ is a zero-order Bessel function and (7b) is the vertical wave equation. It can be shown that $v(z)\propto\partial G/\partial z$ so the solution of (7b) yields the first baroclinic mode. Unfortunately it is not possible to follow Godfrey's (1973b, and private communication) derivation of v since he imposed $G(0)=0$ whereas our data show $G(0)$ is approximately -300 m. This boundary condition is a very significant feature which must be taken into account when mode shapes from this or any other baroclinic instability theory are being calculated for East Australian eddies. At this stage all we can propose is a rudimentary eddy model. Since $v(z)\propto\partial G/\partial z$ we may follow Rhines' (1970) argument for constant N^2 to find that our eddy is the low-frequency limit of an inertio-gravity wave where

$$D\approx|f|/kN=|f|/k(g\Delta\rho/\rho D_0)^{\frac{1}{2}}. \quad (8)$$

This is a general result, but D_0 (the scale depth of the thermocline) is ill-defined; presumably $D<D_0$ but not greatly so. Using $D\sim D_0$ in (8) gives

$$D\approx(f/k)^2/(g\Delta\rho/\rho). \quad (9)$$

The Rossby radius of deformation is

$$\mu=[g(\Delta\rho/\rho)D]^{\frac{1}{2}}/|f| \quad (10)$$

and from (9) this becomes

$$\mu\approx k^{-1}. \quad (11)$$

The real test of our theoretical model is whether μ, defined by (11) and therefore directly measurable from the horizontal scales of our eddy, agrees with Godfrey's value of 39.6 km. Since $\epsilon=J_0(kr)G(z/D)$, the dynamic height of any surface relative to a level of no motion in the abyss is

$$\eta(z,r)=\eta_0 f(z/D)[J_0(kr)-J_0(kR)]/[1-J_0(kR)],\quad 0\leqslant r\leqslant R, \quad (12)$$

where $f(z/D)\rightarrow 0$ as $(z/D)\rightarrow-\infty$ and $f(0)=1$. Eq. (12) is linear in $J_0(kr)$ and arranged so that η_0 is the dynamic relief, η falling to zero at the radius R. The eddy as defined by (12) is a current ring with surface speed

$$v(r)=-(kg\eta_0/f)J_1(kr)/[1-J_0(kR)]. \quad (13)$$

Obviously kR is the first non-zero root of J_1, i.e., $k=3.8317/R$. The eddy diameter was found to be 230 km in Section 6. According to (13) the maximum speed occurs at $r=0.49R$ so a second estimate of eddy diameter is obtained from the diameter of the current ring which was found to be 130 km, i.e., $R=130/(2\times 0.49)=133$ km from the frontal structure and $R=115$ km from the regions of zero horizontal gradient. The average is $R=124$ km so $k=3.09\times 10^{-5}$ m^{-1} and from (11) $\mu=32.4$ km which agrees well with Godfrey's value of 39.6 km, thus verifying the model.

9. Scales of the eddy

Since we now have $R=124$ km and $f=-8.36\times 10^{-5}$ s^{-1} while Godfrey (private communication) has found $\Delta\rho/\rho\approx 2\times 10^{-3}$ and $D_0\approx 500$ m, whereupon D from (8) is about 430 m, we need only calculate η_0 to specify our eddy completely [within the limitation that the form of $f(z/D)$ is uncertain]. Conventionally η_0 may be estimated from (1) in the absence of deep density data. Taking 8°C as the equivalent continuous thermal relief of $T240$ (from the curves of $T240$ and $T400$ on Fig. 6 and noting that the isothermal core extends beyond

240 m) then (1) yields $\eta_0=0.71$ dyn-m. A second estimate of η_0 is found by averaging the computed currents on Fig. 8 (1.05 m s^{-1}) and assuming that this current in the ring is the maximum value predicted by (13). This process yields $\eta_0=0.69$ dyn-m so we may confidently assume $\eta_0 \approx 0.7$ dyn-m.

In establishing the balance of forces we consider the Froude number and the Rossby number. The Froude number is the ratio of the inertial curvature force to the pressure gradient force, i.e.,

$$\mathrm{Fr}=(v^2/l)/(g\eta_0/l)=v^2/g\eta_0. \tag{14}$$

Here v is the azimuthal velocity scale (1.05 m s^{-1}), l is the radial scale (65 km) and $\eta_0=0.7$ dyn-m. Hence $\mathrm{Fr}=0.16$. The Rossby number is the ratio of the inertial curvature force to the Coriolis force, i.e.,

$$\mathrm{Ro}=(v^2/l)/fv=v/fl=0.19. \tag{15}$$

This analysis shows that the stream curvature is 16% as important as the pressure gradient and 19% as important as the Coriolis effect. The inertial forces should therefore be considered in the overall dynamics as the assumption of geostrophy will underestimate the current speed.

10. Discussion

The eddy that we have reported is a winter eddy where the surface mixed layer extends beyond 300 m in the eddy core. This is probably typical of recently formed winter eddies off East Australia as deep mixed layers are frequently found in Boland's (1973) monitoring section (private communication based on all the data). This is the most pronounced feature of our eddy and probably makes warm core eddies off east Australia somewhat unique. The simplicity of the axially symmetric structure allows a basic physical model to be derived by treating the eddy as an inertio-gravity wave. In retrospect this could be expected from Godfrey's (1973a, b) papers on eddy fluctuations off East Australia. However, conventional baroclinic instability theories will not predict the vertical current profile because the assumption of zero vertical velocity near the surface is not realized. It is necessary to take deep stations across such an eddy to determine the shape of the profiles. A new length scale has emerged which appears to be more meaningful than the term "eddy radius." This is the radius to the core of the eddy current which seems to be observationally and theoretically half the eddy radius. The diameter of about 250 km actually found is in agreement with the reviewed diameters of 200 to 250 km.

The successful interpretation of ART surveys to reveal subsurface water masses holds much promise for future tracking of eddies; as they move south their warm cores should become clearer with respect to the peripheral water.

The establishment of a closed ring as distinct from the East Australian Current plus Countercurrent interpretation reinforces the concept that these rings are the rule and not the exception. The dynamic height of 0.7 dyn-m is the largest yet reported for the area and probably resulted from the small station spacing across the eddy. The swiftness of the current in the southern and eastern portion of the eddy is twice that of the traditionally observed southerly nearer the coast.

An interesting feature which is probably tied in with the dynamics of the eddy formation is the entrainment and complete encapsulation of northern water by the deeper shell of 16.75°C water.

Acknowledgments. The authors wish to acknowledge the enthusiastic support of the officers and men of HMAS *Kimbla.* The ART maps were made available to us by Dr. G. Murphy of the CSIRO Division of Fisheries and Oceanography. From the same establishment, Mr. B. V. Hamon and in particular Dr. Stuart Godfrey gave us the benefit of their deep insight into the dynamics of the region, while Fred Boland made available the complete data from the monitoring section across the Tasman Sea. P. Scully-Power acknowledges the generous advice and encouragement he received from Dr. Von Winkle and Charles Brown, Jr., while he was at the Naval Underwater Systems Centre. This work was supported in part by the Office of Naval Research, under Contract N000 14-75-WR50209 for Project ANZUS Eddy.

REFERENCES

Boland, F. M., 1973: A monitoring section across the East Australian Current CSIRO Div. Fish. Oceanogr., Tech. Pap. 34.

——, and Hamon, B. V., 1970: The East Australian Current, 1965–1968. *Deep Sea Res.*, **17**, 777–794.

Bye, J. A. T., 1972: Oceanic circulation south of Australia. *Antarctic Oceanology II, The Australian-New Zealand Sector.* Denis E. Hays, Ed., Amer. Geophys. Union, 95–100.

Fugilister, F. C., 1972: Cyclonic rings formed by the Gulf Stream 1965–66. *Studies in Physical Oceanography*, Vol. 1, Arnold L. Gordon, Ed., Gordon and Breach, 137–168.

Godfrey, J. S., 1973a: On the dynamics of the western boundary current in Bryan and Cox's (1968) numerical model ocean. *Deep-Sea Res.*, **20**, 1043–1058.

——, 1973b: Comparison of the East Australian Current with the western boundary flow in Bryan and Cox's (1968) numerical model ocean. *Deep-Sea Res.*, **20**, 1059–1076.

Hamon, B. V., 1961: Structure of the East Australian Current. CSIRO Div. Fish. Oceanogr., Tech. Pap. 11, 11 pp.

——,1962: The spectrums of mean sea level at Sydney, Coff's Harbour and Lord Howe Island. *J. Geophys. Res.*, **67**, 5147–5155.

——, 1965: The East Australian Current, 1960–64. *Deep-Sea Res.*, **12**, 899–921.

——,1968a: Spectrum of sea level at Lord Howe Island in relation to circulation. *J. Geophys. Res.*, **73**, 6925–6927.

——, 1968b: Temperature structure in the upper 250 metres in the East Australian Current area. *Aust. J. Marine Freshwater Res.*, **19**, 91–99.

——, 1970: Western boundary currents in the south Pacific. *Scientific Exploration of the South Pacific*, Warren S. Wooster, Ed., Nat. Acad. Sci., 50–59.

——, and G. R. Cresswell, 1972: Structure functions and intensities of ocean circulation off east and west Australia. *Aust. J. Marine Freshwater Res.*, **23**, 99–103.

Hynd, J. S., 1969: Isotherm maps for tuna fisherman. *Aust. Fish.*, **28**, No. 7, 13–22.

Kitano, K., 1974: A Kuroshio anticyclonic eddy. *J. Phys. Oceanogr.*, **4**, 670–672.

Lighthill, M. J., 1969: Dynamic response of the Indian Ocean to onset of the southwest Monsoon. *Phil. Trans. Roy. Soc. London*, **265**, 45–92.

Patzert, W. C., 1969: Eddies in Hawaiian waters. Hawaii Inst. Geophys. Rep. HIG-69-8, 51 pp.

Rhines, P., 1970: Edge-, bottom-, and Rossby waves in a rotating stratified fluid. *Geophys. Fluid Dyn.*, **1**, 273–302.

Scully-Power, P. D., 1973: Coral Sea flow budgets in winter. *Aust. J. Marine Freshwater Res.*, **24**, 203–215.

Wyrtki, K., 1962: Geopotential topographies and associated circulation in the western south Pacific ocean. *Aust. J. Marine Freshwater Res.*, **13**, 89–105.